

Radiative Effects in Processes of Diffractive Vector Meson Electroproduction

I. Akushevich

National Center of Particle and High Energy Physics, Bogdanovich str. 153, 220040 Minsk, Belarus, e-mail: aku@hep.by

Received: 12 August 1998

Abstract. The electromagnetic radiative correction to the cross section of the vector meson electroproduction is calculated. Explicit covariant formulae for the observed cross section are obtained. The dependence of the radiative correction on the experimental resolution and on the inelasticity cut is discussed. FORTRAN code DIFFRAD based on both exact (ultrarelativistic) and approximate sets of the formulae for the radiative correction to the cross section is presented. The detailed numerical analysis for kinematical conditions of the recent experiments on the diffractive electroproduction of vector mesons is given.

1 Introduction

The measurement of the cross section of the exclusive vector meson electroproduction can provide information on the hadronic component of the photon and on nature of diffraction. During several years the diffractive production of the vector meson has been the subject of the muonproduction [1,2,3] and electroproduction [4,5,6] experiments. Data analysis of these experiments is considerably affected by the QED radiative effects. At practice the radiative corrections (RC) to the processes of electroproduction are taken into account using codes originally developed for the inclusive case (see ref.[7], for example).

The purpose of this paper is to calculate the electromagnetic correction to experimentally observed cross sections for the kinematics of a fixed target and collider experiments directly. The Feynman diagrams necessary to calculate RC are presented on Fig.1.

In order to calculate exactly the QED RC to the cross section of vector meson production, the method offered in ref.[8] is used. By exact formulae is meant the expressions for the lowest order RC obtained without any approximations but ultrarelativistic: the lepton mass m is considered to be small. In Section 2 the kinematics of the radiative and non-radiative processes and exact formulae for the lowest order RC are obtained. In Section 3 the analytical results are visualized by the construction of the approximate formulae for cases interesting in practice. The numerical results are given in Section 4. A brief discussion and conclusions are given in Section 5.

2 Exact formulae for the lowest order correction

Seven kinematical variables are necessary to describe the radiative process of the diffractive vector meson produc-

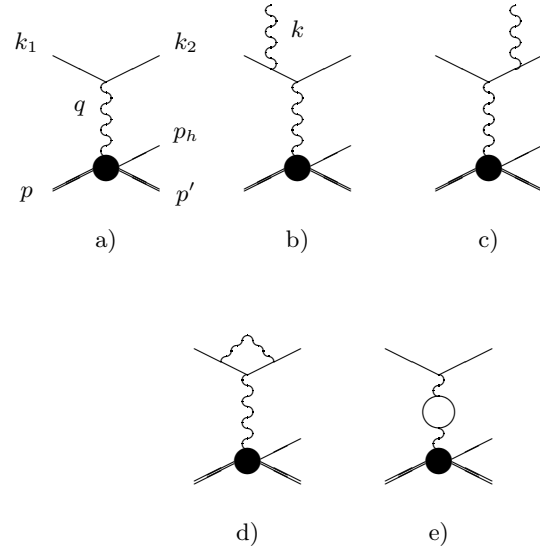


Fig. 1. Feynman diagrams contributing to the Born and the next order cross sections. The letters denote the four-momenta of corresponding particles.

tion (Figure 1b,c). Four of them are the same as for non-radiated case: usual scaling variables x and y , the negative square of momentum transferred from the virtual photon to the proton $t = (q - p_h)^2$ and the angle ϕ_h between the scattering ($\mathbf{k}_1, \mathbf{k}_2$) and production (\mathbf{q}, \mathbf{p}_h) planes in the laboratory frame. The squared virtual photon momentum $Q^2 = -(k_1 - k_2)^2$ and the invariant mass of the initial proton and the virtual photon $W^2 = (p + q)^2$ are often used instead of x and y . The kinematics of a real photon is described by three additional variables: the inelasticity $v = \Lambda^2 - M^2$ (M is the proton mass and

$\Lambda^2 = (p' + k)^2$ is the squared invariant mass of the system of unobserved particles), $\tau = kq/kp$ and angle ϕ_k between planes $(\mathbf{k}_1, \mathbf{k}_2)$ and (\mathbf{q}, \mathbf{k}) .

We consider RC to three and four dimensional cross sections $\sigma = d\sigma/dxdydt d\phi_h$ and $\bar{\sigma} = d\sigma/dxdydt$. They are related as

$$\bar{\sigma} = \int_0^{2\pi} d\phi_h \sigma. \quad (1)$$

The four differential Born cross section can be presented in the form

$$\sigma_0 = \frac{\alpha}{4\pi^2 xy} \left(y^2 \sigma_T + 2 \left(1 - y - \frac{1}{4} y^2 \gamma^2 \right) (\sigma_L + \sigma_T) \right), \quad (2)$$

where σ_T and σ_L are differential cross sections of the photoproduction, $\gamma^2 = Q^2/\nu^2$ and ν is the virtual photon energy.

The differential cross section of the radiative process has the following form:

$$\sigma_R \sim \frac{|M_b + M_c|^2}{4 k_1 p} dv \frac{d^3 k}{2k_0} \delta((\Lambda - k)^2 - M^2), \quad (3)$$

where $\Lambda = p + q - p_h$, $M_{b,c}$ are matrix elements of the processes given in Figure 1b,c. In order to extract the infrared divergence into a separate term we following [8], use the identity

$$\sigma_R = \sigma_R - \sigma_{IR} + \sigma_{IR} = \sigma_F + \sigma_{IR}, \quad (4)$$

where σ_F is finite for $k \rightarrow 0$ and σ_{IR} is the infrared divergent part

$$\sigma_{IR} = \frac{\alpha}{\pi} \delta_R^{IR} \sigma_0 = \frac{\alpha}{\pi} (\delta_S + \delta_H) \sigma_0. \quad (5)$$

The quantities δ_S and δ_H appear after splitting the integration region over v by the infinitesimal parameter \bar{v} :

$$\begin{aligned} \delta_S &= \frac{1}{\pi} \int_0^{\bar{v}} dv \int \frac{d^{n-1} k}{(2\pi\mu)^{n-4} k_0} F_{IR} \delta((\Lambda - k)^2 - M^2), \\ \delta_H &= \frac{1}{\pi} \int_{\bar{v}}^{v_m} dv \int \frac{d^3 k}{k_0} F_{IR} \delta((\Lambda - k)^2 - M^2), \end{aligned} \quad (6)$$

where μ is an arbitrary parameter of the mass dimension, v_m is a maximal inelasticity and

$$F_{IR} = \frac{m^2}{(2kk_1)^2} + \frac{m^2}{(2kk_2)^2} - \frac{Q^2 + 2m^2}{(2kk_1)(2kk_2)}. \quad (7)$$

The way to calculate the integrals like (6) has been offered in ref.[8] (see also review [9]). In our case we have

$$\begin{aligned} \delta_S &= 2 \left(P_{IR} + \log \frac{\bar{v}}{\mu M} \right) (l_m - 1) + \log \frac{S' X'}{m^2 M^2} + S_\phi, \\ \delta_H &= 2(l_m - 1) \log \frac{v_m}{\bar{v}}, \end{aligned} \quad (8)$$

where $l_m = \log(Q^2/m^2)$. The quantities $S' = 2\Lambda k_1 = S - Q^2 - V_1$ and $X' = 2\Lambda k_2 = X + Q^2 - V_2$ are calculated using $V_{1,2} = 2(a_{1,2} + b \cos \phi_h)$, where

$$\begin{aligned} a_1 &= \frac{1}{2\lambda_q} (Q^2 S_p S_t - (S S_x + 2M^2 Q^2) t_q), \\ a_2 &= \frac{1}{2\lambda_q} (Q^2 S_p S_t - (X S_x - 2M^2 Q^2) t_q), \\ b &= \frac{1}{\lambda_q} (Q^2 S_t^2 - S_t S_x t_q - M^2 t_q^2 - m_v^2 \lambda_q)^{1/2} \\ &\quad \times (S X Q^2 - M^2 Q^4 - m^2 \lambda_q)^{1/2}. \end{aligned} \quad (9)$$

The invariants are defined as

$$\begin{aligned} S &= 2k_1 p, \quad X = 2k_2 p = (1 - y)S, \quad Q^2 = Sxy, \\ S_{p,x} &= S \pm X, \quad S_t = S_x + t, \quad t_q = t + Q^2 - m_v^2, \\ \lambda_q &= S_x^2 + 4M^2 Q^2. \end{aligned} \quad (10)$$

The infrared terms P_{IR} , parameters μ and \bar{v} as well as the squared logarithms containing the mass singularity l_m^2 are completely canceled in the sum of δ_R^{IR} with δ_V coming from a contribution of the vertex function (Figure 1d):

$$\delta_V = -2(P_{IR} + \log \frac{m}{\mu})(l_m - 1) - \frac{1}{2} l_m^2 + \frac{3}{2} l_m - 2 + \frac{\pi^2}{6}. \quad (11)$$

For this sum we have

$$\delta_S + \delta_H + \delta_V = \delta_{inf} + \delta_{VR}, \quad (12)$$

where

$$\delta_{VR} = \frac{\alpha}{\pi} \left(\frac{3}{2} l_m - 2 - \frac{1}{2} \log^2 \frac{X'}{S'} + \text{Li}_2 \left[1 - \frac{Q^2 M^2}{S' X'} \right] - \frac{\pi^2}{6} \right),$$

$$\delta_{inf} = \frac{\alpha}{\pi} (l_m - 1) \log \frac{v_m^2}{S' X'}. \quad (13)$$

Here the ultrarelativistic expression for S_ϕ calculated in [10] was used. The higher order corrections can be partially taken into account using a special procedure of exponentiation of the multiple soft photon radiation. There is an uncertainty, what part of δ_{VR} has to be exponentiated. Within the considered approach [10] $(1 + \delta_{inf})$ is replaced by $\exp \delta_{inf}$.

For the observed cross section of the vector meson electroproduction we obtain

$$\sigma_{obs} = \sigma_0 e^{\delta_{inf}} (1 + \delta_{VR} + \delta_{vac}) + \sigma_F. \quad (14)$$

The correction δ_{vac} comes from the effects of vacuum polarization by leptons and hadrons (Figure 1e). The explicit QED formulae for the first one can be found in ref.[11]. The hadronic contribution is given by a fit coming from the data on $e^+ e^- \rightarrow \text{hadrons}$ [12].

The contribution of the infrared finite part can be written in terms of POLRAD 2.0 notation [11,13]:

$$\begin{aligned} \sigma_F &= -\frac{\alpha^2 y}{16\pi^3} \int_0^{2\pi} d\phi_k \int_{\tau_{min}}^{\tau_{max}} d\tau \sum_{i=1}^2 \sum_{j=1}^3 \theta_{ij} \times \\ &\quad \times \int_{\bar{v}}^{v_m} \frac{dv}{f} R^{j-2} \left[\frac{\mathcal{F}_i}{Q^4} - \delta_j \frac{\mathcal{F}_i^0}{Q^4} \right], \end{aligned} \quad (15)$$

where $R = v/f$, $f = 1 + \tau - \mu$ and $2M\tau_{max,min} = S_x \pm \sqrt{\lambda_q}$; $\delta_j = 1$ for $j = 1$ and $\delta_j = 0$ otherwise.

The quantities θ_{ij} depend only on the kinematical invariants and the integration variables τ and ϕ_k

$$\begin{aligned}\theta_{11} &= 4Q^2 F_{IR}^0, \\ \theta_{12} &= 4\tau F_{IR}^0, \\ \theta_{13} &= -2(2F + F_d\tau^2), \\ \theta_{21} &= 4(SX - M^2Q^2)F_{IR}^0, \\ \theta_{22} &= -F_dS_p^2\tau + F_{1+}S_pS_x + 2F_{2-}S_p \\ &\quad - 4F_{IR}^0M^2\tau + 2F_{IR}^0S_x, \\ \theta_{23} &= 4FM^2 + 2F_dM^2\tau^2 - F_dS_x\tau - F_{1+}S_p,\end{aligned}\quad (16)$$

where

$$F_d = \frac{F}{z_1z_2}, F_{1+} = \frac{F}{z_1} + \frac{F}{z_2}, F_{2\pm} = F\left(\frac{m^2}{z_2^2} \pm \frac{m^2}{z_1^2}\right), \quad (17)$$

$F = 1/(2\pi\sqrt{\lambda_q})$ and $F_{IR}^0 = F_{2+} - Q^2F_d = F_{IR}R^2$. The quantities $\mu = kp_h/kp = 2(a_k + b_k \cos(\phi_h - \phi_k))$ and $z_{1,2} = kk_{1,2}/kp = 2(a_{1,2}^z - b^z \cos \phi_k)$ include the dependence on angles:

$$\begin{aligned}a_1^z &= \frac{1}{2\lambda_q}(Q^2S_p + \tau(SS_x + 2M^2Q^2)), \\ a_2^z &= \frac{1}{2\lambda_q}(Q^2S_p + \tau(XS_x - 2M^2Q^2)), \\ a_k &= \frac{1}{2\lambda_q}((2Q^2 + \tau S_x)S_m - (S_x - 2\tau M^2)t_q), \\ b^z &= \frac{1}{\lambda_q}(SXQ^2 - M^2Q^4 - m^2\lambda_q)^{1/2} \\ &\quad \times (Q^2 + \tau S_x - \tau^2 M^2)^{1/2}, \\ b_k &= \frac{1}{\lambda_q}(Q^2S_m^2 - S_mS_xt_q - M^2t_q^2 - m_v^2\lambda_q)^{1/2} \\ &\quad \times (Q^2 + \tau S_x - \tau^2 M^2)^{1/2}.\end{aligned}\quad (18)$$

Here $S_m = S_t - v$.

The dependence on the photoproduction cross sections is included in \mathcal{F}_i :

$$\begin{aligned}\mathcal{F}_1 &= (S_x - R)\sigma_T^R, \quad \mathcal{F}_2 = \frac{2\tilde{Q}^2}{S_x - R}(\sigma_T^R + \sigma_L^R), \\ \mathcal{F}_1^0 &= S_x\sigma_T, \quad \mathcal{F}_2 = 2x(\sigma_T + \sigma_L).\end{aligned}\quad (19)$$

The quantities $\sigma_{T,L}$ have to be calculated for Born kinematics, but $\sigma_{T,L}^R$ is calculated in terms of so called true kinematics. It means that they have to be calculated for the tilde variables

$$\begin{aligned}\tilde{Q}^2 &= Q^2 + R\tau, \\ \tilde{W}^2 &= W^2 - R(1 + \tau), \\ \tilde{t} &= t + R(\tau - \mu)\end{aligned}\quad (20)$$

instead of usual Q^2 , W^2 and t .

The important point is the dependence of the results on the maximal inelasticity v_m . The inelasticity is calculated in terms of the measured momenta, so it is possible

to make a cut on the maximal value of this quantity. If this cut is not applied the maximal inelasticity is defined by kinematics only. Below we give the formulae for v_m in terms of the kinematical invariants

$$4Q^2v_m = \left(\sqrt{\lambda_q} - \sqrt{t_q^2 + 4m_v^2Q^2}\right)^2 - (S_x - 2Q^2 + t_q)^2 - 4M^2Q^2 \quad (21)$$

and in terms of kinematical limits on t

$$v_m = \frac{1}{C}(t_{max} - t)(t - t_{min}), \quad (22)$$

where C behaves for small t as

$$C = \frac{Q^2 + m_v^2}{2W^2}(S_x + \sqrt{\lambda_q}) + O(t). \quad (23)$$

The maximal inelasticity given by kinematics are plotted in Figure 2.

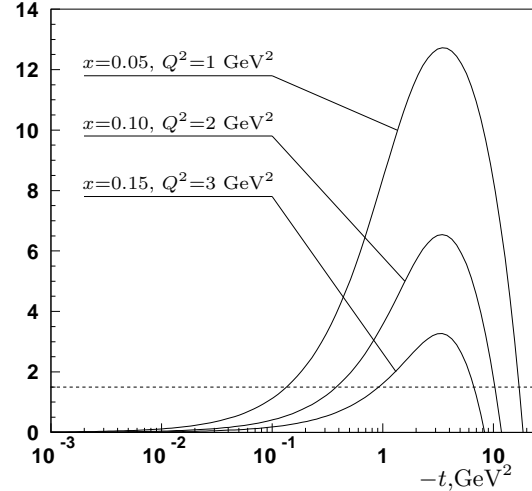


Fig. 2. Maximal inelasticity within kinematical conditions of HERMES. Dashed line gives a possible cut.

3 The approximation

The structure of the exact formulae for the cross section of the hard bremsstrahlung σ_F obtained in the last section is not simple. Here we analyze them under approximation. The third integration variable v is not completely photonic one. It is calculated from the measured momenta of the final lepton and the vector meson. For non-radiated events $v \equiv 0$. At practice, however the distribution over v has a Gaussian form due to the finite resolution. Radiative effects also affect the distribution (see sect. 4.3). So a cut

on the invariant mass of the unobserved system rejects events with hard radiated photon and helps to reduce the total RC. Below we consider the approximation based on assumption that v_m is relatively small or kinematical cut on v is used. Besides, for the diffractive scattering the squared momentum t transferred to the hadronic system is always small, so we construct the approximate formulae for RC to the cross section $d\sigma/dx dy dt$ with an additional assumption

$$M^2 \ll S; t \ll Q^2. \quad (24)$$

It is clear that this condition is normal for the collider experiments but it is often not so bad for fixed target experiments as well. Due to the smallness of v_m we can keep only leading term in the expansion of integrand (15) over v . First non-vanishing term contains the first derivative of the integrand. The main contribution to this derivative comes from $\exp(b_v t)$ (b_v is a slope parameter). It is not difficult to keep all the contributions to the derivative but for simplicity we restrict our calculation to this contribution. In this case

$$\frac{1}{v} \left[\frac{Q^4}{\bar{Q}^4} \frac{\mathcal{F}_i}{\mathcal{F}_i^0} - 1 \right] \approx b_v \frac{\tau - \mu}{1 + \tau - \mu} \quad (25)$$

and it is possible to integrate over ϕ_h , ϕ_k and τ explicitly:

$$\begin{aligned} \frac{1}{2\pi} \int_0^{2\pi} d\phi_h \frac{\tau - \mu}{1 + \tau - \mu} &\approx \frac{Q^2 + m_v^2}{S_x - Q^2 - m_v^2}, \\ \int_0^{2\pi} d\phi_k \int_{\tau_{min}}^{\tau_{max}} d\tau F_{IR}^0 &= -2(l_m - 1). \end{aligned} \quad (26)$$

Final result for $\bar{\sigma}_F$ (see eq.(1)) is simple

$$\bar{\sigma}_F = \frac{2\alpha b_v v_m}{\pi} (l_m - 1) \frac{Q^2 + m_v^2}{S_x - Q^2 - m_v^2} \bar{\sigma}_0. \quad (27)$$

Apart from a simple analytical form the obtained formula has one more advantage. The correction depends only on the kinematical variables but not on the dynamical characteristics of the interaction like σ_T and σ_L . It allows to eliminate a possible systematical error coming from the choice of the model. Such systematics could be large because we have to know the differential cross sections σ_T and σ_L in the wide region of varying of four variables, but there are neither enough experimental data for that nor satisfactory models. Using (27) we have systematics coming from the using of the approximate formulae instead of exact ones. But we are able to control it by comparing the values calculated by (15) and (27) using any model.

Moreover there is a possibility to provide the procedure 'event by event' reweighting each event with the RC factor. The comparison of the results for the cross sections with and without this reweighting gives the correction.

4 Numerical analysis and code DIFFRAD

In this section we present the FORTRAN code DIFFRAD created on the basis of the exact formulae performed in

Section 2. The program calculates the lowest order RC to the diffractive vector meson electroproduction. The higher order effects are approximated by the procedure of exponentiation. The formulae for the cross section are given in a covariant form, so the code can be run both for the fixed target experiments and for the experiments at collider. The model for $\sigma_{L,T}$ presented originally in ref.[14] and developed in ref.[15] is used as an input.

Below we give numerical results for RC factor

$$\eta = \frac{\bar{\sigma}_{obs}}{\bar{\sigma}_0} = \frac{\int_0^{2\pi} d\phi_h \sigma_{obs}}{\int_0^{2\pi} d\phi_h \sigma_0} \quad (28)$$

and t - and v -distributions obtained within the kinematical regions of recent experiments on the electro- and muon-production of vector mesons.

4.1 RC to the cross section

On Figure 3 one can see Q^2 -and t -dependences of RC factor η in the kinematical region of experiments of EMC and NMC. There is no cut on inelasticity used. For high values of t the RC can reach factor two. The reason of so large effect is smallness of the Born photoproduction cross sections $\sigma_{L,T}$. They fall as $\exp(b_v t)$. In the observed cross section this factor is under integral and there is a contribution from the region on t where $\sigma_{L,T}$ are not so small. As a result σ_{obs} falls with the increasing $-t$ but not so fast.

Figure 4 gives the results for η within kinematics of the experiment E665 with a cut on the inelasticity. Notice it can be done because of the rather good resolution over v (standard deviation σ of its distribution is more smaller than v_m given by kinematics). The usage of this cut leads to a different behavior of η as a function of Q^2 .

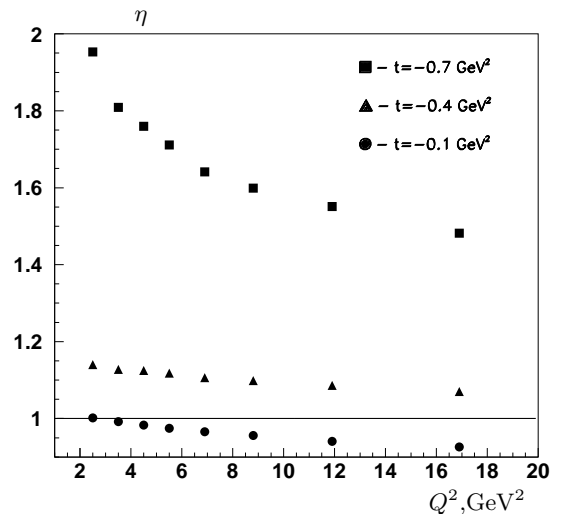


Fig. 3. RC factor in kinematical conditions of EMC/NMC ($\mu p \rightarrow \mu p p$).

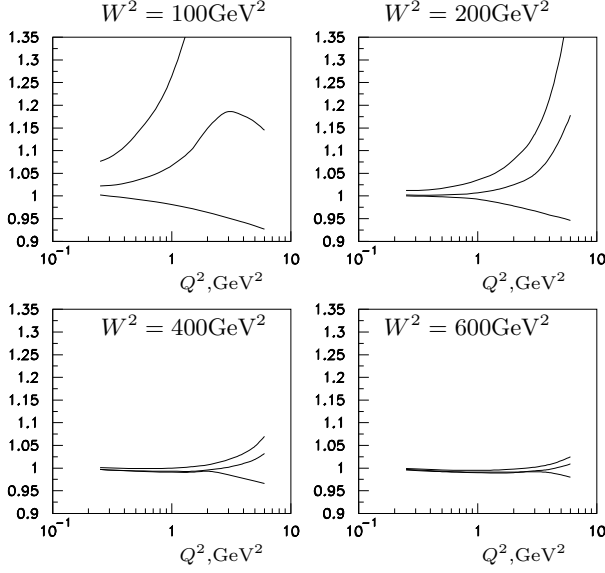


Fig. 4. RC factor in kinematical conditions of E665 ($\mu p \rightarrow \mu p p$). Curves from top to bottom correspond to $t = -0.9, -0.5, -0.1$ GeV^2 .

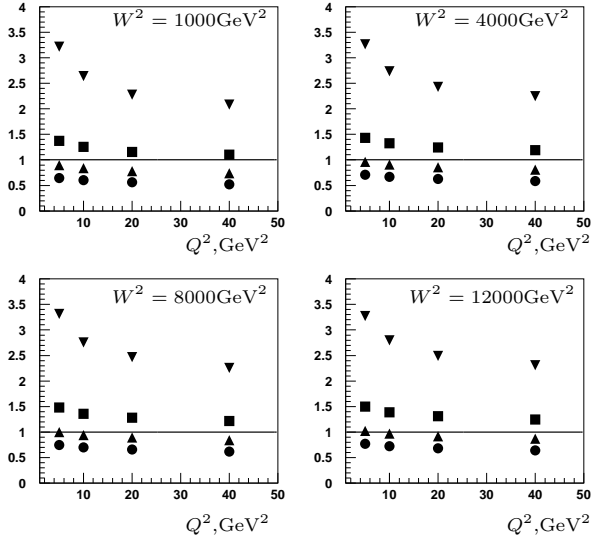


Fig. 5. RC factor in kinematical conditions of collider experiments at HERA ($ep \rightarrow e p p$). Symbols from top to bottom correspond to $t = -0.7, -0.5, -0.3, -0.1$ GeV^2

The different plots on this figure give W^2 -dependence of η .

The dependence of η on the kinematical variables Q^2 , W^2 and t in the region of the collider experiments at HERA is presented in Figure 5. No cut on inelasticity is used, so Q^2 -dependence is similar to one given for the EMC/NMC experiment. It is found that the RC factor η is not sensitive for W^2 . It is due to the fact that the photo-production cross section is almost flat in the kinematical region of the collider experiments.

The dependence on the v_m cut in the region of HERMES kinematics is analyzed in Figure 6. The usage of the

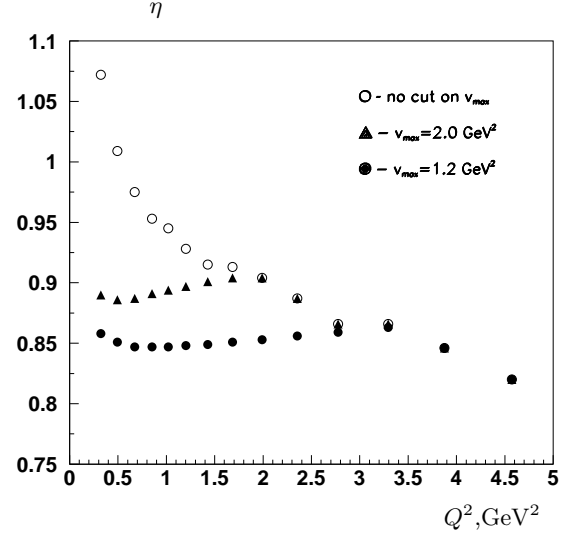


Fig. 6. RC factor in kinematical conditions of HERMES ($ep \rightarrow e p p$).

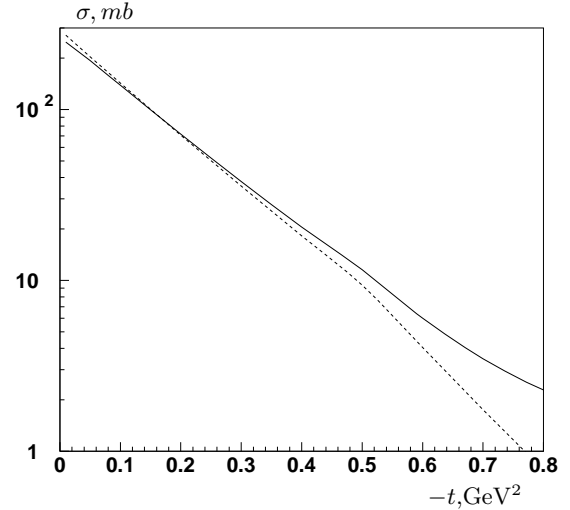


Fig. 7. The Born (dashed) and observed (solid) cross sections in respect to $-t$. No cut on inelasticity is used.

cut changes RC factor for small Q^2 and does not influence on the RC for larger values of Q^2 . It can be understood from Figure 2. In the case of the cut usage we have to define v_m as a minimum of the value of the cut and v_m given by the kinematical restrictions (21). For fixed values of $-t$ the cut influence on v_m and RC till certain value of Q^2 only.

4.2 t -distribution

The radiative effects can influence on the slope of the observed cross section in respect to $-t$ due to essential dependence of RC on this variable. It is illustrated in Figures

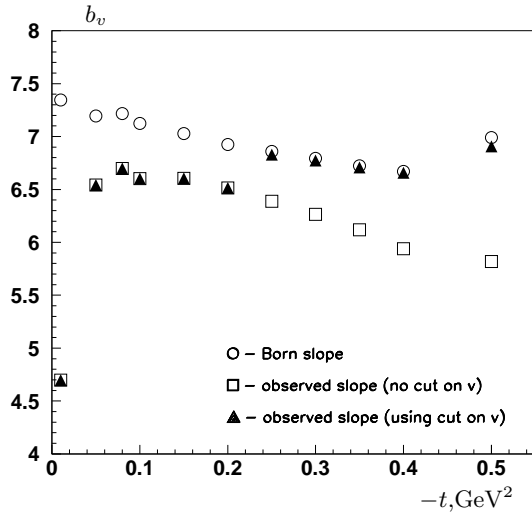


Fig. 8. Slope parameter in respect to $-t$

7 and 8. The t -dependence of the Born cross section within the model of refs. [14,15] is basically defined by two-gluon formfactor taken in exponential form $\exp(b_v t)$ with $b_v = 5$. The dependence on p_t also influences on the slope of the Born cross section in respect to $-t$. An additional dependence on t in the case of RC comes basically from v_m , that is proportional to $t - t_{min}$ in the diffractive region of small $-t$. Due to this fact both exponent $\exp(\delta_{inf})$ and the cross section σ_F tend to zero when $t \rightarrow t_{min}$. So the observed cross section vanishes in this limit.

4.3 Inelasticity distribution

There are several reasons for the inelasticity to be non-zero: the finite experimental resolution, the mixture of non-exclusive events and radiative effects. In this paper we assume that a special procedure of separation of exclusive and non-exclusive events has been performed. Strictly speaking such procedure can suppress radiative effects partially. It depends on the details of data processing of a concrete experiment, and we assume for simplicity that there are no such suppression.

Figure 9 gives two distribution: Born (pure Gaussian with a zeroth mean value coming from the effects of a finite experimental resolution) and with taking into account RC. The second distribution consists of events of two types. First ones come from the Born, loop and radiated events with $v < \sigma$. This distribution have the same mean value ($v = 0$) and σ as the Born distribution. Other part of the events in the radiative corrected distribution comes from the radiated events with $v > \sigma$. Total number of two distributions is the same.

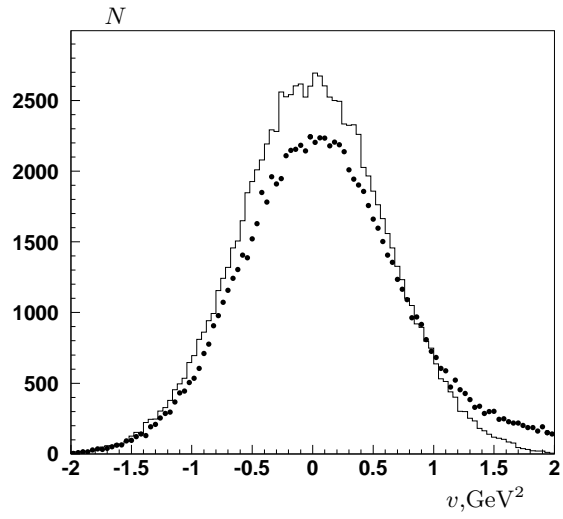


Fig. 9. Inelasticity distributions: Born (line) and radiatively corrected (circles)

5 Discussion and Conclusion

In this article the QED radiative effects have been analyzed in kinematics of recent experiments on the exclusive vector meson electroproduction. The explicit covariant formulae for RC to the cross section are given in eqs.(13-15). An approximate expression for the bremsstrahlung cross section can be found in eq.(27).

The RC to the cross section of the diffractive vector meson electroproduction is very sensitive to the cut on the inelasticity. Using harder cut leads to smaller values of RC factor.

In the diffractive region ($-t < 0.3$) RC is negative and can reach

- 10% for muon experiments with fixed target;
- 20% for electron experiments with fixed target;
- 40% for electron collider experiments.

This large effect comes basically from a double logarithmic contribution in δ_{inf} (13). For example for collider kinematics both its logarithms exceed 10, and δ_{inf} can reach 0.5.

There are no essential dependence on the type of a vector meson. All numerical results are given for the case of ρ meson production. The dependence on the type of a scattered lepton is typical. RC in the case of the electron scattering is several times more due to the appearing the lepton mass in the argument of the leading logarithm.

The observed cross section has steeper slope in respect to t than the Born cross section. RC to the slope parameter is negative and $\sim 10\%$.

FORTTRAN code DIFFRAD is available (aku@hep.by) for the calculation of RC to observable quantities in experiments on the diffractive vector meson electroproduction.

Acknowledgements

I am grateful to A.Brull and N.Shumeiko for help and support. Also I would like to thank N.Akopov, A.Borisov, A.Droutskoi, P.Kuzhir, A.Nagaitsev, M.Ryskin, A.Soroko and H.Spiesberger for fruitful discussions and comments.

References

1. EMC Collaboration, J.J. Aubert et al., Phys. Lett. **B161**, (1985) 203.
2. NMC Collaboration (M. Arneodo et al.) Nucl. Phys. **B429**, (1994) 503.
3. E665 Collaboration; (M.R. Adams et al.), Diffractive Production of ρ (770) Mesons in Muon-Proton Interactions at 470-GeV., MPI-PHE-97-03, Feb 1997. 28pp.
4. H1 Collaboration; S. Aid et al., Nucl. Phys. **B468**, (1996) 3.
5. ZEUS Collaboration; M.Derrick et al., Phys. Lett. **B356**, (1995) 601.
6. HERMES Collaboration; M.Tytgat for the collaboration, Vector Meson Production at HERMES, Proceedings of the DIS98 Workshop, Brussels, Belgium, April 1998, World Scientific. (*to be published*)
7. K.Kurek, DESY 96-209, 1996, hep-ph/9606240.
8. D.Yu.Bardin, N.M.Shumeiko, Nucl. Phys. **B127**, (1977) 242.
9. A.Akhundov, D.Bardin, L.Kalinovskaya, T.Riemann, Fortsch. Phys. **44**, (1996) 373.
10. N.M.Shumeiko, Sov. J. Nucl. Phys. **29**, (1979)807.
11. I.V.Akushevich and N.M.Shumeiko, J.Phys. **G20**, (1994) 513.
12. H.Burkhardt, B.Pietrzyk, Phys.Lett. **B356**, (1995)398.
13. I.Akushevich, A.Ilyichev, N.Shumeiko, A.Soroko, A.Tolkachev, Comp. Phys. Comm. **104**, (1997)201.
14. M.G. Ryskin, Z.Phys. **C57**, (1993) 89.
15. M. Arneodo, L. Lamberti, M. Ryskin, Comp. Phys. Comm. **100**, (1997) 195.